

# Regulator of G Protein Signaling Protein Suppression of $G\alpha_o$ Protein-Mediated $\alpha_{2A}$ Adrenergic Receptor Inhibition of Mouse Hippocampal CA3 Epileptiform Activity

Brianna L. Goldenstein, Brian W. Nelson, Ke Xu, Elizabeth J. Luger, Jacqueline A. Pribula, Jenna M. Wald, Lorraine A. O'Shea,<sup>1</sup> David Weinshenker, Raelene A. Charbeneau, Xinyan Huang, Richard R. Neubig, and Van A. Doze

*Department of Pharmacology, Physiology and Therapeutics, University of North Dakota, School of Medicine and Health Sciences, Grand Forks, North Dakota (B.L.G., B.W.N., K.X., E.J.L., J.A.P., J.M.W., L.A.O., V.A.D.); Department of Human Genetics, Emory University, Atlanta, Georgia (D.W.); and Department of Pharmacology, University of Michigan, Medical School, Ann Arbor, Michigan (R.A.C., X.H., R.R.N.)*

Received December 18, 2008; accepted February 18, 2009

## ABSTRACT

Activation of G protein-coupled  $\alpha_2$  adrenergic receptors (ARs) inhibits epileptiform activity in the hippocampal CA3 region. The specific mechanism underlying this action is unclear. This study investigated which subtype(s) of  $\alpha_2$ ARs and G proteins ( $G\alpha_o$  or  $G\alpha_i$ ) are involved in this response using recordings of mouse hippocampal CA3 epileptiform bursts. Application of epinephrine (EPI) or norepinephrine (NE) reduced the frequency of bursts in a concentration-dependent manner: (-)EPI > (-)NE >>> (+)NE. To identify the  $\alpha_2$ AR subtype involved, equilibrium dissociation constants ( $pK_b$ ) were determined for the selective  $\alpha$ AR antagonists atipamezole (8.79), rauwolscine (7.75), 2-(2,6-dimethoxyphenoxyethyl)aminomethyl-1,4-benzodioxane hydrochloride (WB-4101; 6.87), and prazosin (5.71). Calculated  $pK_b$  values correlated best with affinities determined previously for the mouse  $\alpha_{2A}$ AR subtype ( $r = 0.98$ , slope = 1.07). Furthermore, the inhibitory effects of EPI were lost in

hippocampal slices from  $\alpha_{2A}$ AR- but not  $\alpha_{2C}$ AR-knockout mice. Pretreatment with pertussis toxin also reduced the EPI-mediated inhibition of epileptiform bursts. Finally, using knock-in mice with point mutations that disrupt regulator of G protein signaling (RGS) binding to  $G\alpha$  subunits to enhance signaling by that G protein, the EPI-mediated inhibition of bursts was significantly more potent in slices from RGS-insensitive  $G\alpha_o^{G184S}$  heterozygous ( $G\alpha_o$ +GS) mice compared with either  $G\alpha_{i2}^{G184S}$  heterozygous ( $G\alpha_{i2}$ +GS) or control mice ( $EC_{50} = 2.5$  versus 19 and 23 nM, respectively). Together, these findings indicate that the inhibitory effect of EPI on hippocampal CA3 epileptiform activity uses an  $\alpha_{2A}$ AR/ $G\alpha_o$  protein-mediated pathway under strong inhibitory control by RGS proteins. This suggests a possible role for RGS inhibitors or selective  $\alpha_{2A}$ AR agonists as a novel antiepileptic drug therapy.

This work was supported by the North Dakota Experimental Program to Stimulate Competitive Research through the National Science Foundation (NSF) [Grant EPS-0447679]; NSF Faculty Early Career Development Award [Grant 0347259]; NSF Research Experience for Undergraduates Site [Grant 0639227]; NSF Research Experience for Teachers [Grant 0639227]; National Institutes of Health National Institute on Drug Abuse [Grant 5-R01-DA17963]; National Institutes of Health National Institute of General Medical Sciences [Grant 5-R01-GM039561]; and National Institutes of Health National Center for Research Resources INBRE Program [Grant P20-RR016741].

Preliminary reports of these findings were presented at the 2007 annual meeting of the American Society for Biochemistry and Molecular Biology (ASBMB) Northwest Regional Undergraduate Affiliate Network; 2007 October 26–27; Moorhead, MN; and the 2008 annual meetings of the ASBMB and the American Society for Pharmacology and Experimental Therapeutics, 2008 April 5–9, San Diego, CA.

B.L.G. and B.W.N. contributed equally to this work.

<sup>1</sup> Current affiliation: Schroeder Middle School, Grand Forks, North Dakota. Article, publication date, and citation information can be found at <http://molpharm.aspetjournals.org>. doi:10.1124/mol.108.054296.

The noradrenergic system modulates many physiological and pathological processes within the central nervous system (CNS). Noradrenergic neurons regulate attention and arousal, sleep, and learning and memory (Pupo and Minneman, 2001) and seem to attenuate epileptic activity (Giorgi et al., 2004). The hippocampus receives substantial noradrenergic innervation in all regions, including the cornu ammonis 3 (CA3), a region essential for many cognitive functions such as spatial pattern recognition, novelty detection, and short-term memory (Kesner et al., 2004). The CA3 region possesses a dense recurrent network of excitatory axons between the pyramidal neurons that may be crucial for performing these

**ABBREVIATIONS:** CNS, central nervous system; ACSF, artificial cerebral spinal fluid; AR, adrenergic receptor; CA3, cornu ammonis 3; EPI, epinephrine; GPCR, G-protein coupled receptor; KO, knockout; NE, norepinephrine; RGS, regulator of G-protein signaling; WB-4101, 2-(2,6-dimethoxyphenoxyethyl)aminomethyl-1,4-benzodioxane hydrochloride; WT, wild type; PTX, pertussis toxin; JP-1302, *N*-[4-(4-methyl-1-piperazinyl)phenyl]-9-acridinamine dihydrochloride.

cognitive functions but also makes the region vulnerable to overexcitation (Schwartzkroin, 1986). This region has one of the lowest seizure thresholds and is often involved in temporal lobe epilepsy, the most common human epileptic syndrome. It is clear that thoroughly delineating the inhibitory and excitatory aspects of this region is critical to understanding CNS function and dysfunction and to designing targeted therapeutic approaches.

Norepinephrine (NE) is the major neurotransmitter released by noradrenergic neurons and modulates several CA3 processes. NE has been shown to facilitate long-term potentiation, which is involved in memory formation, and antiepileptic activity (Giorgi et al., 2004) in the hippocampal CA3 region. Increased NE release in the brain has been shown to inhibit epileptiform activity, whereas reduced NE levels seem to increase seizure susceptibility (Weinshenker and Szot, 2002). Although the mechanism by which NE mediates these effects is still unclear, NE may both potentiate memory and inhibit the overexcitation associated with seizures (Jurgens et al., 2005) through the distinct and diverse expression of postsynaptic receptor subtypes (Hillman et al., 2005).

Adrenergic receptors (ARs) are divided into three major classes, each of which has a unique G protein pairing resulting in diverse physiological actions (Pupo and Minneman, 2001). Studies have suggested that  $\beta$ ARs mediate the enhancement of long-term potentiation (Hopkins and Johnston, 1988) and memory (Devauges and Sara, 1991), whereas the antiepileptogenic actions of NE may involve  $\alpha_2$ AR activation (Giorgi et al., 2004). Pharmacological and molecular cloning studies have revealed the existence of three  $\alpha_2$ AR subtypes denoted  $\alpha_{2A}$ ,  $\alpha_{2B}$ , and  $\alpha_{2C}$  (Bylund et al., 1994). We recently showed that NE inhibits rat hippocampal CA3 epileptiform bursts through  $\alpha_{2A}$ AR activation (Jurgens et al., 2007). Furthermore, specific activation of  $\alpha_{2A}$ ARs attenuates seizures in mice elicited by chemoconvulsants (Szot et al., 2004).

ARs are part of a large and diverse family of GTP-binding (G) protein-coupled receptors (GPCRs). The extracellular signals received by GPCRs are relayed by heterotrimeric G proteins ( $G\alpha\beta\gamma$ ) to effector enzymes and channels within the cell (Gilman, 1987). The conversion of GDP-bound inactive  $G\alpha\beta\gamma$  heterotrimer into activated  $G\alpha$ -GTP and  $G\beta\gamma$  subunits is achieved by catalyzing nucleotide exchange on  $G\alpha$  subunits via GPCR activation. Once released, the subunits interact with a variety of downstream effectors in an intracellular signaling cascade (Offermanns, 2003). Deactivation of the G protein is achieved by hydrolysis of the  $G\alpha$ -bound GTP, a step that controls the duration of the signal. The GDP-bound  $G\alpha$  subunit will then reform with the  $G\beta\gamma$  heterodimer, forming an inactive trimer once again.

For some  $G\alpha$  families ( $G_{i/o}$  and  $G_q$ ), the rate of GTP hydrolysis can be enhanced by regulator of G protein signaling (RGS) proteins (Berman et al., 1996; Watson et al., 1996). Consequently, RGS proteins are negative modulators of signaling through receptors coupled to the  $G_{i/o}$  and  $G_q$  family of G proteins (Clark et al., 2008) and enhance intrinsic GTPase activity of the GTP-bound  $G\alpha$  subunits. This GTPase acceleration attenuates G protein signaling by resetting the  $G\alpha$  subunit to its inactive conformation (Hollinger and Hepler, 2002). Interfering with the activity of RGS proteins allows the  $G\alpha$  subunit to remain active for a longer time, effectively enhancing the signal (Lan et al., 1998; Clark et al., 2003). Therapeutic agents targeting RGS proteins could be used to

enhance the effect of current GPCR-mediated drug therapies by reducing the required therapeutic dose while increasing the regional agonist specificity, thereby decreasing the possibility of side effects (Zhong and Neubig, 2001; Neubig and Siderovski, 2002).

This study investigated the role of  $\alpha_2$ ARs and RGS proteins in the antiepileptic actions of NE using field recordings of hippocampal CA3 epileptiform burst activity and a combination of selective blockers for the AR and G protein subtypes, transgenic  $\alpha_2$ AR knockout, and RGS-insensitive  $G\alpha$  subunit knock-in mice. Delineating which  $\alpha_2$ AR and G protein subtypes are involved in attenuating hippocampal epileptiform activity will help to further elucidate the mechanism by which NE inhibits epileptogenesis and may suggest potential targets for antiepileptic drug therapy.

## Materials and Methods

### Reagents

Atipamezole was made by Orion Corporation (Espoo, Finland). Desipramine, L(-)-epinephrine (+)-bitartrate, L(-)-norepinephrine (+)-bitartrate, D-(+)-norepinephrine (-)-bitartrate, oxymetazoline hydrochloride, pertussis toxin, picrotoxin, pindolol, and timolol maleate were obtained from Sigma-Aldrich (St. Louis, MO). Prazosin hydrochloride, rauwolscine hydrochloride, and WB-4101 were acquired from Tocris Cookson Inc. (Ellisville, MO). All chemical reagents used to make the artificial cerebrospinal fluid (ACSF) were of biological grade from J. T. Baker, Inc. (Phillipsburg, NJ) or Thermo Fisher Scientific (Waltham, MA). Isoflurane was purchased from Abbott Diagnostics (Chicago, IL).

### Animals

C57BL/6J mice of both genders were used in the present study. Mice were housed two to four per cage (size 11.5 × 7 inches) under standard laboratory conditions on a 12-h light/dark cycle (lights on at 7:00 AM) in rooms maintained at a temperature of ~22°C with a relative humidity of ~55%. Water and dried laboratory food (Teklad Global 18% Protein Rodent Diet; Harlan Teklad, Madison, WI) were provided ad libitum. Mice were allowed to acclimate for at least 4 days after arrival (see below). All protocols described were approved by the Institutional Animal Care and Use Committee of Emory University (Atlanta, GA), the University of Michigan (Ann Arbor, MI), and the University of North Dakota (Grand Forks, ND) in accordance with National Institute of Health guidelines (Institute of Laboratory Animal Resources, 1996) and meet the guidelines of the American Association for Accreditation of Laboratory Animal Care.

### Transgenic Mice

**Generation of  $\alpha_{2A}$ AR- and  $\alpha_{2C}$ AR-Knockout Mice.**  $\alpha_{2A}(-/-)$  [ $\alpha_{2A}/\alpha_{2C}; (-/-)/(+/+)$ ] and  $\alpha_{2C}(-/-)$  [ $\alpha_{2A}/\alpha_{2C}; (+/+)/(-/-)$ ] mice, maintained on a pure C57BL/6J background, were generated at Emory University using heterozygous  $\alpha_{2C}(+/-)$  and  $\alpha_{2AC}(+/-)$  mice obtained from Brian K. Kobilka (Stanford University, Stanford, CA). Genotypes were confirmed by polymerase chain reaction. All mice were reared in a specific pathogen-free facility at Emory University with a 12-h light/dark cycle (lights on at 7:00 AM) and were shipped to the University of North Dakota at age 2 to 5 months. Control animals used in these studies were wild-type (WT) C57BL/6J [ $\alpha_{2A}/\alpha_{2C}; (+/+)/(+/+)$ ] mice purchased from The Jackson Laboratory (Bar Harbor, ME).

**Generation of  $G\alpha_o^{G184S}$  Heterozygous ( $G\alpha_o$ +/GS) Knock-In Mice.** The original  $G\alpha_o^{G184S}$  ES cell line, described in Fu et al. (2004, 2006), was developed in a 129-D3 ES cell background, which never went germline. Consequently, the  $G\alpha_o^{G184S}$  mouse strain was constructed from a 129-CJ7 ES line using methods similar to those previously reported for the  $G\alpha_{i2}^{G184S}$  strain (Fu et al., 2006; Huang

et al., 2006). Specifically, we prepared a targeting construct by restriction digestion to obtain DNA fragments of the mouse *Gnao* gene from a Bac clone derived from 129-CJ7 DNA Bac library (ResGen; Invitrogen, Carlsbad, CA). Using those fragments, a targeting construct was prepared in the TKLNL vector (Mortensen et al., 1992). First the mutant  $G\alpha_o$  exon 5 was produced by mutating the sequence AAAACAACCTGGC ATCGTAGAAA to AAAACAACCTAGTATCGTAGAAA. The bases in boldface type indicate the changed codon (Gly<sup>184</sup> to Ser<sup>184</sup>), and the underline portion designates the location of the resulting diagnostic SpeI restriction site. This mutated exon 5 and additional 5' genomic sequence to form the "left" homology arm was cloned into TKLNL to introduce the loxP-flanked neo marker after exon 5, then the right arm genomic fragment from exons 6 to 8 was cloned 3' of the loxP cassette in a manner similar to that for preparing the  $G\alpha_{i2}^{G184S}$  targeting vector (Fu et al., 2006; Huang et al., 2006). CJ7 ES cells were electroporated with the targeting vector, and homologous recombinants were isolated. Targeted CJ7 ES cells were microinjected into C57BL/6Ncr1 × (C57BL/6J × DBA/2J)F1 mouse blastocysts to generate ES cell-mouse chimeras. After identification of chimeric offspring, the mice were backcrossed onto a C57BL/6J background for at least four generations. Only heterozygous offspring of crosses between  $G\alpha_o(+/G184S)$  male and C57BL/6J female mice (N4-N5) were used in these studies because homozygous  $G\alpha_o(G184S/G184S)$  offspring from heterozygous × heterozygous crosses were not viable. Control animals used in these studies were WT littermates [(+/+)] of the  $G\alpha_o^{G184S}$  heterozygous ( $G\alpha_o+/GS$ ) mice.

**Generation of  $G\alpha_{i2}^{G184S}$  Heterozygous ( $G\alpha_{i2}+/GS$ ) Knock-In Mice.**  $G\alpha_{i2}^{G184S}$  heterozygous ( $G\alpha_{i2}+/GS$ ) knock-in mice, maintained on a pure C57BL/6J background (>10 generations), were generated at the University of Michigan, Ann Arbor, as described previously (Fu et al., 2006). All genotypes were confirmed by polymerase chain reaction. Control animals used in these studies were WT C57BL/6J mice from The Jackson Laboratory. Both the  $G\alpha_o^{G184S}$  and  $G\alpha_{i2}^{G184S}$  heterozygous (+/GS) knock-in mice were reared at the University of Michigan and were confirmed to be pathogen-free before their shipping to the University of North Dakota at age 1 to 3 months.

### Hippocampal Slice Preparation

After being deeply anesthetized with isoflurane, mice weighing 16 to 27 g were decapitated, and their brains were rapidly removed. The hippocampi were then quickly dissected from each hemisphere and placed into an ice-cold Ringer solution containing 110 mM choline chloride, 2.5 mM KCl, 7 mM MgSO<sub>4</sub>, 0.5 mM CaCl<sub>2</sub>, 1.25 mM NaH<sub>2</sub>PO<sub>4</sub>, 25 mM NaHCO<sub>3</sub>, 25 mM D-glucose, 11.6 mM sodium ascorbate, and 3.1 mM sodium pyruvate, saturated with 95% O<sub>2</sub>/5% CO<sub>2</sub>. Using a conventional tissue sectioning apparatus (Stoelting, Wood Dale, IL), the hippocampi were sliced transversely into 500- $\mu$ m thick sections and transferred to ACSF consisting of 119 mM NaCl, 5 mM KCl, 1.3 mM MgSO<sub>4</sub>, 2.5 mM CaCl<sub>2</sub>, 1 mM NaH<sub>2</sub>PO<sub>4</sub>, 26.2 mM NaHCO<sub>3</sub>, and 11 mM D-glucose, which was continually aerated with 95% O<sub>2</sub>/5% CO<sub>2</sub>. The slices were incubated at 32 ± 1°C for 30 min, then transferred to room temperature (22 ± 1°C) and allowed to recover for at least 30 min before experimentation.

### Electrophysiological Recordings

A single slice was transferred to the recording chamber, where it was submerged and superfused continuously at a rate of at least 4 ml/min with ACSF at room temperature. Glass microelectrodes were made using a vertical two-stage puller (PP-830; Narishige, Tokyo, Japan). Extracellular field potentials were recorded using microelectrodes filled with 3 M NaCl placed in the stratum pyramidale of the CA3 region of the hippocampus using an SZ-61 stereo microscope (Olympus, Melville, NY). Potentials were detected using either an Axoclamp 2B (Molecular Devices, Sunnyvale, CA) or BVC-700A (Dagan, Minneapolis, MN) microelectrode amplifier, amplified using a Brownlee 440 signal conditioner (Brownlee Precision, San Jose, CA),

digitized with a Digidata 1322A analog-to-digital converter (Molecular Devices), and recorded using Axoscope 9.0 software (Molecular Devices).

### Generation of Epileptiform Activity

Hippocampal CA3 pyramidal neurons are prone to spontaneously firing epileptiform bursts partly as a result of their extensive associational connections (Schwartzkroin, 1986). This activity was easily generated by superfusing the slice with ACSF containing 100  $\mu$ M picrotoxin, a GABA<sub>A</sub> receptor blocker, to attenuate synaptic inhibition. If no burst discharges were seen after 30 min of superfusion, the slice was determined to be unresponsive and discarded. Once continuous spontaneous epileptiform burst discharges were evident, 30 min of baseline data were recorded before any exposure to an AR agonist. The ACSF also contained 0.5  $\mu$ M desipramine to block NE transporters [i.e., potential reuptake of the catecholamines epinephrine (EPI) and NE] and 30  $\mu$ M timolol to block any  $\beta$ AR-mediated excitatory effects (Jurgens et al., 2005), as well as any applicable  $\alpha$ AR antagonist. Before being used, each AR antagonist was tested to ensure that it possessed no independent effects. Preliminary experiments also confirmed that each AR agonist concentration caused its maximal effect during an 8-min application (data not shown). Because the  $\alpha_2$ AR antagonist rauwolscine also has potent serotonergic 5-hydroxytryptamine<sub>1A</sub> receptor-mediated agonist activity (Newman-Tancredi et al., 1998), we substituted 3  $\mu$ M pindolol (which blocks both  $\beta$ AR and 5-hydroxytryptamine<sub>1A</sub> receptors) for timolol (which only blocks  $\beta$ ARs) when using this particular  $\alpha_2$ AR antagonist.

### Data Analysis

Epileptiform burst discharge frequencies were visualized in real time (Fig. 1A) while being recorded for subsequent analysis. Postexperimental analysis was completed using Mini Analysis 6.0 software (Synaptosoft, Decatur, GA). The last interval correlating to each agonist concentration was noted, the baseline frequency was subtracted, and that value was used to plot a concentration-response expressed as a percentage of maximal response. Frequency versus agonist concentration data were then entered into Prism 5.0 software (GraphPad Software Inc., San Diego, CA), and concentration-response curves were constructed using a nonlinear least-squares curve-fitting method. Each curve was fitted with a standard (slope = unity) or variable slope, and the best fit was determined using an *F* test with a value of *p* < 0.05. The calculated EC<sub>50</sub> value was used as a measurement of agonist potency. Significance between groups was compared statistically using the Student's *t* test (*p* < 0.05).

Schild analysis was used to determine the apparent equilibrium dissociation constants (pK<sub>b</sub>) for selective  $\alpha$ AR antagonists (Arunlakshana and Schild, 1959). For each experiment, cumulative concentration-response curves were performed in adjacent slices from the same mouse (one dose-response curve per slice). Dose ratios of EC<sub>50</sub> values were calculated in the presence and absence of a selective  $\alpha_2$ AR antagonist and Schild plots constructed by graphing the log of the dose ratio - 1 versus the log of the antagonist concentration. Linear regression analysis of these points was used to determine the slope and *x*-intercept. Schild regression slopes are given as mean ± S.E. and were considered to be nonunity if the 95% confidence interval did not include the value of 1. The pK<sub>b</sub> values of  $\alpha$ AR antagonists causing competitive inhibition of the EPI-mediated reduction in burst frequencies were calculated from Schild regression *x*-intercepts. Differences in pK<sub>b</sub> values and Schild regression slopes were determined by analysis of covariance with a *p* < 0.05 level of probability accepted as significant. EC<sub>50</sub> and pK<sub>b</sub> values are expressed as the mean ± S.E. for *n* experiments.

## Results

**Effects of EPI and NE on Mouse CA3 Epileptiform Activity.** We first examined the effects of EPI on mouse CA3



epileptiform burst discharges in the presence of timolol ( $\beta$ AR blockade) to elucidate the action of  $\alpha$ AR activation on hippocampal activity. Picrotoxin-induced epileptiform burst discharges are shown in Fig. 1, and their frequency is reduced by application of EPI in a concentration-dependent manner. For this particular experiment, the  $EC_{50}$  value calculated from nonlinear regression analysis was 48 nM. Our previous work in rats has shown that this effect is most likely mediated by an  $\alpha_2$ AR in the CA3 region of the hippocampus (Jurgens et al., 2007). As illustrated in Fig. 2, the rank order of potency of the three AR agonists tested in this manner revealed that (-)EPI ( $31 \pm 8.1$  nM,  $n = 45$  slices) > (-)NE ( $150 \pm 45$  nM,  $n = 15$  slices) >>> (+)NE ( $4700 \pm 3300$  nM,  $n = 10$  slices), which is consistent with our previous results (Jurgens et al., 2007) and the order expected for  $\alpha$ ARs.

**Effects of the Selective  $\alpha_2$ AR Antagonist Atipamezole and Subtype-Selective  $\alpha_2$ AR Antagonists on the EPI-Mediated Decrease in Burst Discharge Frequencies.** Functional determination of equilibrium dissociation constant ( $K_b$ ) value for selective  $\alpha$ AR antagonists was used to characterize the type of  $\alpha$ AR mediating decreased burst frequency in the hippocampal CA3 region. Pretreatment of hippocampal slices with 3, 10, and 30 nM atipamezole produced 2-, 6-, and 22-fold parallel rightward shifts of the fitted EPI concentration-response curve (Fig. 3A). The  $pK_b$  of 8.79 ( $n = 5$ ) for atipamezole (Fig. 3B) was similar to previously published binding  $pK_i$  values for the mouse  $\alpha_2$ ARs (Link et al., 1992; Chruscinski et al., 1992; see also Table 1). This result suggests that the response is mediated by an  $\alpha_2$ AR.

Subtype-selective antagonists were then used to determine

the specific subtype of  $\alpha_2$ AR mediating burst frequency reduction in the mouse hippocampal CA3 region. Apparent  $pK_b$  values of subtype-selective  $\alpha_2$ AR competitive antagonists were determined using Schild regression analysis. Slices pretreated with either prazosin ( $\alpha_{2B}$ AR-selective), rauwolscine ( $\alpha_{2C}$ AR-selective), or WB-4101 ( $\alpha_{2C}$ AR-selective) produced parallel rightward shifts of the fitted EPI concentration-response curve in all instances (data not shown). For each of these selective  $\alpha_2$ AR antagonists, the slope of the regression line was close to the value of unity. The logs of the equilibrium dissociation constants ( $pK_b$ ) calculated for these  $\alpha_2$ AR antagonists were as follows: rauwolscine (7.75,  $n = 3$ ), WB-4101 (6.87,  $n = 3$ ), and prazosin (5.71,  $n = 4$ ) (Table 1).

**$\alpha_2$ AR Antagonist Functional  $pK_b$  Estimates Correlate to  $\alpha_{2A}$ AR  $pK_i$  Values.** A method often used to compare equilibrium dissociation constants of many receptor antagonists is to correlate  $pK_b$  values with previously published  $pK_i$  values (Bylund, 1988). Both the correlation coefficient and slope of the correlation line should be close to unity if the calculated functional values correspond to the published binding constants for a specific receptor. Illustrated in Fig. 4 are the correlations between the  $pK_b$  values determined for the selective  $\alpha$ AR antagonists used in this study and the previously published  $pK_i$  values of these AR antagonists for each mouse  $\alpha_2$ AR subtype (Table 1). For the mouse  $\alpha_{2A}$ AR subtype, a very high correlation coefficient ( $r = 0.98$ ) along with a slope similar to unity (slope = 1.07) were calculated for our experimental  $pK_b$  values compared with published binding affinity values (Fig. 4A). In contrast, for the mouse  $\alpha_{2B}$ AR, a poor correlation coefficient ( $r = 0.88$ ) and low slope

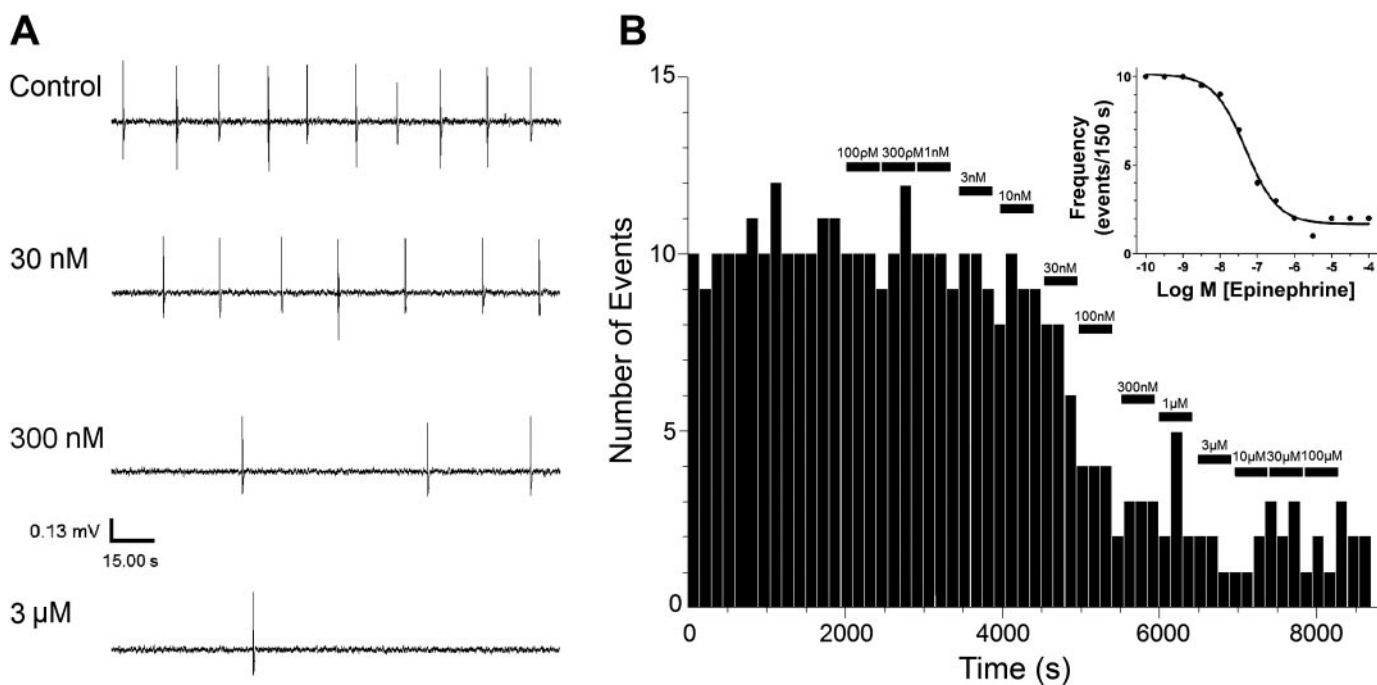


**Fig. 1.** Effects of EPI on mouse hippocampal CA3 epileptiform activity. **A**, continuous 150-s long chart recordings of burst discharges recorded in the hippocampal CA3 region of brain slices from WT mice. Epileptiform burst discharges were elicited by including 100  $\mu$ M concentration of the GABA $_A$  receptor blocker picrotoxin in the perfusing ACSF containing 30  $\mu$ M timolol and 0.5  $\mu$ M desipramine. Under these conditions, bath application of EPI reduced burst frequency in a concentration-dependent manner from 10 bursts (0.067 Hz) in control Ringer solution to 7 (0.047 Hz) in 30 nM EPI, 3 (0.020 Hz) in 300 nM EPI, and 1 (0.007 Hz) in 3  $\mu$ M EPI. **B**, frequency histogram of the number of burst discharges versus time of EPI application. Each bin represents the frequency averaged over an approximately 150-s epoch. Increasing concentrations of EPI were applied to the bath for the 8-min periods indicated. Inset, concentration-response curve derived from the frequency histogram. Data points were plotted as the percentage of maximal inhibition (decrease in epileptiform burst frequency), and the curve was constructed using a nonlinear least-squares curve-fitting method. For this experiment, the concentration-response curve was fit best by a nonvariable sigmoidal model with a calculated  $EC_{50}$  value for EPI of 48 nM.

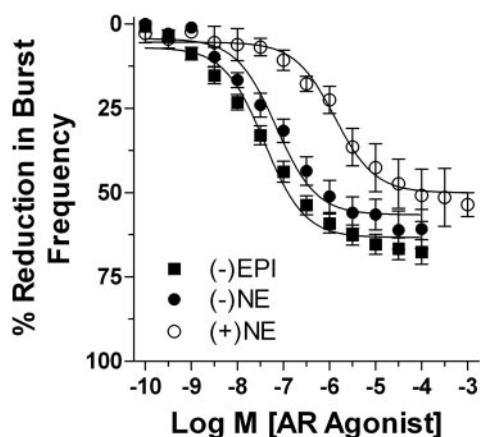


**Fig. 2.** Potency for EPI and NE inhibiting hippocampal CA3 epileptiform burst activity. Extracellular field potential recordings were used to generate concentration-response curves using increasing amounts of (-)EPI (■), (-)NE (●), and (+)NE (○) in the presence of 100  $\mu$ M picrotoxin, 30  $\mu$ M timolol, and 0.5  $\mu$ M desipramine. There was a significant difference in the potencies ( $EC_{50}$  values) calculated for (-)EPI ( $31 \pm 8.1$  nM,  $n = 45$  slices from 18 animals), (-)NE ( $150 \pm 45$  nM,  $n = 15$  slices from 7 animals), and (+)NE (4700  $\pm$  3300 nM,  $n = 10$  slices from 4 animals). Concentration-response curves for each agonist were plotted as a percentage of decrease (reduction) in epileptiform burst frequency. Each individual experiment best fit to a nonvariable sigmoidal curve. There was no significant difference in the efficacy of (-)EPI ( $68 \pm 2.6\%$ ), (-)NE ( $67 \pm 3.7\%$ ), and (+)NE ( $58 \pm 7.2\%$ ) at reducing epileptiform activity.

(slope = 0.40) were observed when comparing our experimental  $pK_b$  values with previously published  $pK_i$  values (Fig. 4B). Likewise for the mouse  $\alpha_{2C}AR$ , a poor correlation coefficient ( $r = 0.89$ ) and low slope (slope = 0.63) were seen (Fig. 4C). These results suggest that the  $\alpha_{2A}AR$  is the predominant

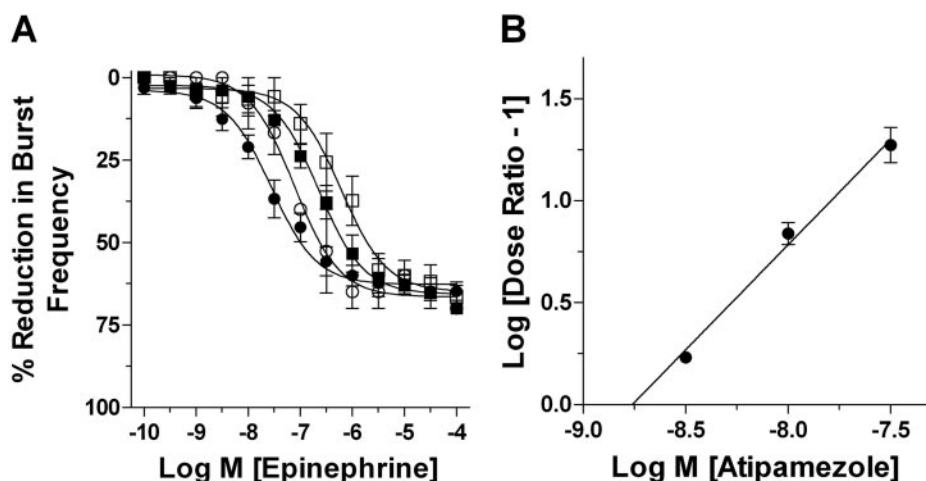


**Fig. 3.** Schild regression analysis using the selective  $\alpha_2AR$  antagonist atipamezole. A, consecutive EPI concentration-response curves demonstrate a concentration-dependent effect of the selective  $\alpha_2AR$  antagonist, atipamezole, on the EPI-mediated inhibition of hippocampal CA3 epileptiform activity in brain slices from WT mice. Pretreatment with 3 nM (●), 10 nM (■), and 30 nM (□) concentrations of this antagonist produced consecutive parallel rightward shifts of the EPI curve that were significantly different from control (●) ( $EC_{50} = 76 \pm 3$ ,  $218 \pm 30$ , and  $762 \pm 274$ , respectively, versus  $34 \pm 12$  nM for control). B, using dose ratios calculated from individual experiments illustrated in A, a Schild plot was created generating a regression slope equaling  $1.06 \pm 0.12$  and an  $x$ -intercept correlating to a  $pK_b$  value of 8.79,  $n = 5$  animals (see Table 1).

**TABLE 1**

Comparisons of experimental functional  $pK_b$  values with binding affinity  $pK_i$  values for selective  $\alpha AR$  antagonists for mouse  $\alpha_2AR$  subtypes  $pK_b$  values represent the negative logarithm<sub>10</sub> of the  $K_b$ , and are expressed as the mean. Schild regression slopes are expressed as the mean slope  $\pm$  S.E. and were determined in three to five separate experiments using brain slices from WT mice. Reported  $pK_i$  values are from binding affinity studies using recombinant mouse  $\alpha_2AR$  clones expressed in COS-7 cells.  $pK_b$  value was calculated using a single 10  $\mu$ M concentration of JP-1302.

Antagonist	$pK_b$	Slope	Reported $pK_i$ Values		
			$\alpha_{2A}AR$	$\alpha_{2B}AR$	$\alpha_{2C}AR$
Atipamezole	8.79	$1.06 \pm 0.12$	$9.07^a$	$8.30^b$	$8.80^a$
Rauwolscine	7.75	$1.01 \pm 0.07$	$7.27^a$	$8.14^b$	$9.10^a$
WB-4101	6.87	$0.89 \pm 0.08$	$6.58^a$	$7.15^b$	$8.11^a$
Prazosin	5.71	$0.97 \pm 0.06$	$5.67^a$	$7.23^b$	$7.01^a$

<sup>a</sup> Link et al. (1992).

<sup>b</sup> Chruscinski et al. (1992).

subtype mediating the antiepileptic action of EPI in mouse hippocampus.

**Effects of EPI on Epileptiform Activity in Slices from  $\alpha_{2A}AR$ - and  $\alpha_{2C}AR$ -Knockout Mice.** To confirm our pharmacological results, we examined the effects of EPI on hippocampal CA3 epileptiform activity in  $\alpha_{2A}AR$ - and  $\alpha_{2C}AR$ -knockout (KO) mice. As illustrated in Fig. 5, EPI was applied in increasing concentrations to hippocampal brain slices prepared from either  $\alpha_{2A}AR$ - or  $\alpha_{2C}AR$ -KO mice. The potency of EPI in the  $\alpha_{2C}AR$ -KO mouse line ( $37 \pm 12$  nM,  $n = 15$ ) fit best with a unity-slope sigmoidal model and was not significantly different from the WT mice (see also Fig. 2). In contrast, the effects of EPI were largely abolished in brain slices from  $\alpha_{2A}AR$ -KO mice with a maximum effect of less than 10% inhibition. These results demonstrate that the  $\alpha_{2A}AR$  is the predominant receptor subtype mediating the inhibitory effects of EPI in the mouse hippocampus.

**Effects of Subtype-Selective  $\alpha_{2A}AR$  Antagonist Oxymetazoline on the EPI-Mediated Decrease in Burst Discharge Frequencies in  $\alpha_{2C}AR$ -KO Mice.** To further evaluate a potential role for  $\alpha_{2B}AR$ s and confirm that the response was primarily an  $\alpha_{2A}AR$  response, the selective  $\alpha_{2A}AR$  antagonist oxymetazoline was used in brain slices made from  $\alpha_{2C}AR$ -KO mice.  $\alpha_{2C}AR$ -KO mouse slices that had been pretreated with 100, 300, and 1000 nM oxymetazoline produced 6-, 22-, and 70-fold parallel rightward shifts of the fitted EPI concentration-response curve (Fig. 6A). The Schild regression slope was  $1.16 \pm 0.12$  and the  $x$ -intercept correlating to a  $pK_b$  value of 7.50 ( $n = 7$  animals) (Fig. 6B). The mouse  $\alpha_{2A}AR$  reported a  $pK_i$  value of 7.49 matched closely to our  $pK_b$  value, whereas the  $\alpha_{2B}AR$  and  $\alpha_{2C}AR$  reported  $pK_i$

values of 5.92 (Chruscinski et al., 1992) and 6.96 (Link et al., 1992) did not. If the  $\alpha_{2B}$ AR made a significant contribution, the slope of the Schild plot should have been less than 1. These results further confirm that this response is primarily mediated by an  $\alpha_{2A}$ AR.

**Effects of Pertussis Toxin on EPI-Mediated Inhibition of CA3 Epileptiform Activity.** Pertussis toxin (PTX) blocks the receptor-mediated activation of G $_{i/o}$  proteins. We used PTX to assess which G protein types are involved in the inhibitory effects of EPI. Extracellular field potential recordings of epileptiform burst frequency were used to generate concentration-response curves using increasing amounts of EPI in untreated control slices or in slices treated with 5  $\mu$ g/ml PTX for 7 to 8 h. As illustrated in Fig. 7, the mean concentration-response curve for nontreated control slices was fit best by a unity-slope sigmoidal model with a calculated EC $_{50}$  value of 12  $\pm$  3.9 nM and a maximum effect of 74  $\pm$  6.1% ( $n$  = 13 slices). Conversely, for PTX-treated slices from the same mice, the mean concentration-response curve showed minimal inhibition (<25%) ( $n$  = 12 slices). These results indicate that inhibition of mouse hippocampal CA3 epileptiform activity in response to EPI is mediated by either G $_i$  or G $_o$  proteins and not G $_s$  or G $_q$  proteins.

**EPI-Mediated Inhibition of CA3 Epileptiform Activity in Slices from G $\alpha_o^{G184S}$  Heterozygous (G $\alpha_o$ +/GS) and G $\alpha_{i2}^{G184S}$  Heterozygous (G $\alpha_{i2}$ +/GS) Knock-in Mice.** To determine a potential role of RGS proteins in the regulation of this response and which type of inhibitory G protein may be involved, we used mice with a knock-in G $\alpha$  subunit mutation (G184S) that renders G $\alpha_o$  and G $\alpha_{i2}$  proteins incapable of binding to the RGS protein. This results in the loss of RGS-mediated inhibition of the G $\alpha_o$  and G $\alpha_{i2}$  protein and enhances G $\alpha$ -specific effects in tissues with responses under RGS control. An increase in response with one of these RGS-insensitive G proteins would implicate that G protein as contributing to the response and RGS proteins as negative regulators. As before, WT control, G $\alpha_o$ +/GS, or G $\alpha_{i2}$ +/GS slices were pretreated with the GABA blocker picrotoxin,  $\beta$ AR blocker timolol, and NE transporter reuptake inhibitor desipramine. Extracellular field potential recordings were used to generate concentration-response curves using increasing amounts of EPI. Inhibition of frequency burst discharges was significantly more potent in brain slices from G $\alpha_o$  mice, with an EC $_{50}$  of 2.5  $\pm$  0.9 nM ( $n$  = 23 slices) versus litter mate control mice (EC $_{50}$  = 19  $\pm$  5 nM,  $n$  = 21 slices) (Fig.

8A). In contrast, there was no significant difference in G $\alpha_{i2}$  mice (EC $_{50}$  = 19  $\pm$  5 nM,  $n$  = 32 slices) compared with the WT controls (EC $_{50}$  = 23  $\pm$  7 nM,  $n$  = 22 slices) (Fig. 8B). These results indicate the EPI-mediated inhibition of mouse hippocampal CA3 epileptiform activity involves a G $\alpha_o$  mechanism under strong negative regulation by RGS proteins.

## Discussion

The role of catecholamines in seizures and epilepsy is complicated, but it is clear that endogenous EPI and NE can protect against many types of seizures (Weinshenker and Szot, 2002). Agonists at all three types of AR ( $\beta$ ,  $\alpha_1$ , and  $\alpha_2$ ) can be antiepileptic, but the most consistent findings show that  $\alpha_2$ AR agonists are generally anticonvulsant, and selective  $\alpha_2$ AR antagonists are proconvulsant (Weinshenker and Szot, 2002). Consequently, we focused the current study on the hippocampus, which plays an important role in the common clinical condition of temporal lobe seizures, to begin to dissect mechanisms underlying the antiepileptic actions of  $\alpha_2$ AR agonists. We used both pharmacological and mouse genetic models to define the receptor and G protein involved in the EPI-mediated antiepileptiform activity in the hippocampus. We have confirmed the role of the  $\alpha_{2A}$ AR in inhibition of hippocampal CA3 epileptiform activity in mice, as shown previously by a pharmacological approach in rats (Jurgens et al., 2007). We built upon these findings by demonstrating that this involves a PTX-sensitive G $_{i/o}$ -type G protein. Furthermore, using RGS-insensitive G $\alpha$  subunit mutant knock-in mice, we show that endogenous RGS protein action on G $\alpha_o$  strongly suppresses this signal, implicating G $\alpha_o$  as a mediator of the response. In contrast, G $\alpha_{i2}$  seems not to be involved. These findings enhance our understanding of the mechanism underlying  $\alpha_{2A}$ AR-mediated inhibition of hippocampal epileptiform activity by NE and suggest a novel approach to antiepileptic drug therapies.

The  $\alpha_{2A}$ AR is the predominant  $\alpha_2$ AR in the CNS, and it has been implicated as the primary anticonvulsant  $\alpha_2$ AR in rat hippocampus in vitro (Jurgens et al., 2007) and in mouse in vivo (Janumpalli et al., 1998). A previous study using dopamine  $\beta$ -hydroxylase,  $\alpha_{2A}$ AR, and  $\alpha_{2C}$ AR-KO mice showed that the proconvulsant effects of  $\alpha_2$ AR agonists were mediated by the  $\alpha_{2A}$ AR autoreceptor, which decreases NE release, whereas the anticonvulsant effects of  $\alpha_2$ AR agonists were

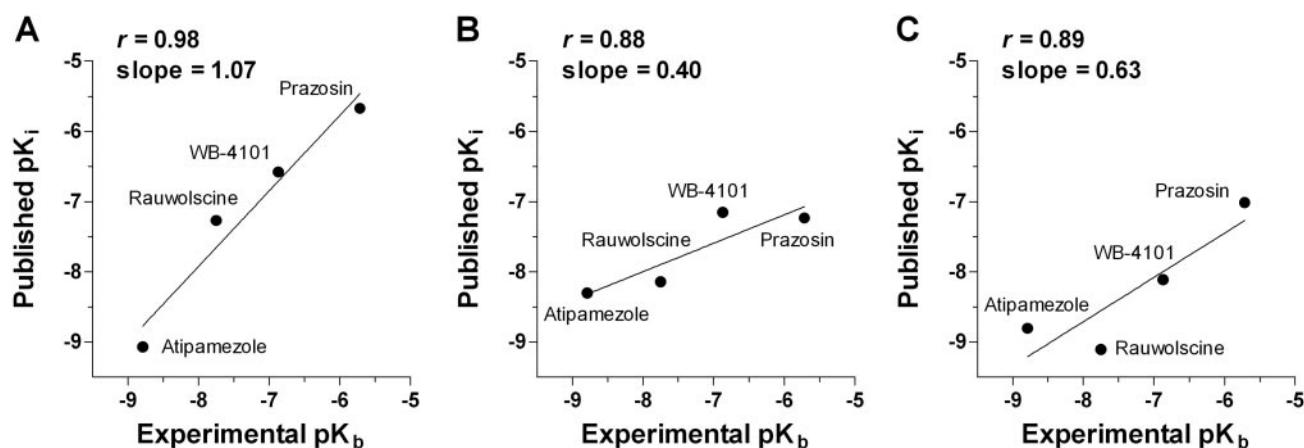


**Fig. 4.** Correlation between the functional affinity estimates ( $pK_b$ ) to the equilibrium dissociation constants ( $pK_i$ ) for various selective  $\alpha_2$ AR antagonists. Using the  $pK_b$  and  $pK_i$  values from Table 1, correlation analyses were performed for the  $\alpha_{2A}$ AR (A), the  $\alpha_{2B}$ AR (B), and the  $\alpha_{2C}$ AR (C).



mediated by  $\alpha_{2A}$ ARs on target neurons (Szot et al., 2004). In the present study, we confirm the results of these findings in mouse using both pharmacological (antagonist  $pK_b$ ) and genetic ( $\alpha_{2A}$ AR- and  $\alpha_{2C}$ AR-KO) approaches. Despite expression of the  $\alpha_{2C}$ AR in hippocampus, it does not seem to contribute at all to the antiepileptiform activity of EPI and NE (Fig. 5). Likewise, the  $\alpha_{2B}$ AR does not seem to play a role (Fig. 6). Neither were  $\alpha_1$ ARs involved in this particular response (Fig. 3 and Table 1). This level of receptor subtype-specificity does not, however, provide any significant therapeutic advance on its own, because the  $\alpha_{2A}$ AR is also the

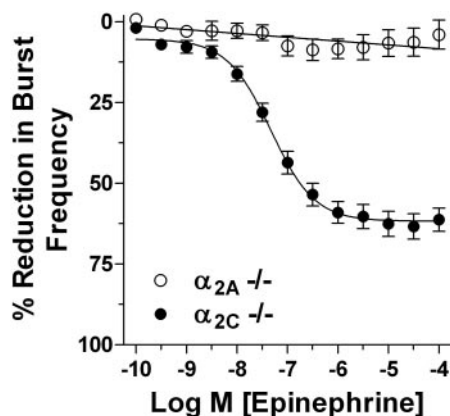


**Fig. 5.** Effects of EPI on hippocampal CA3 epileptiform activity in brain slices from  $\alpha_{2A}$ AR- and  $\alpha_{2C}$ AR-KO mice. Extracellular field potential recordings of epileptiform burst frequency were used to generate concentration-response curves using increasing amounts of EPI in the presence of 100  $\mu$ M picrotoxin, 30  $\mu$ M timolol, and 0.5  $\mu$ M desipramine. Concentration-response curves for EPI were plotted as a percentage of decrease (reduction) in epileptiform burst frequency. For the  $\alpha_{2A}$ AR-KO mice, the mean concentration-response curve for 41 slices from 12 animals was fit best by a linear regression line. In contrast, the mean concentration-response curve for 39 brain slices from 15  $\alpha_{2C}$ AR-KO mice was fit best by a nonvariable sigmoidal model with a calculated  $EC_{50}$  value of  $37 \pm 12$  nM, which was not significantly different from the potency of  $31 \pm 8.1$  nM calculated for EPI in slices from WT mice (see Fig. 2). The efficacy of EPI at reducing the frequency of epileptiform bursts in slices from  $\alpha_{2C}$ AR-KO mice was  $64 \pm 3.9\%$ , which was significantly different from the  $8.7 \pm 3.3\%$  inhibition for EPI in slices from  $\alpha_{2A}$ AR-KO mice.

major receptor involved in the antihypertensive therapeutic effect of  $\alpha_2$ AR agonists and in their major sedative side effect as well (MacMillan et al., 1998). Thus, we pursued subsequent steps in the downstream signaling.

The  $\alpha_2$ ARs are known to couple primarily to  $G_{i/o}$  family G proteins with subsequent actions on several effector systems, including inhibition of adenylyl cyclase, inhibition of voltage-gated calcium channels, and activation of G protein-coupled inwardly rectifying  $K^+$  currents (Offermanns, 2003). The  $G_{i/o}$  protein family is also strongly regulated by the 20-plus member RGS protein family (Neubig and Siderovski, 2002), which has been implicated as a potential drug target (Zhong and Neubig, 2001; Roman et al., 2007). We first confirmed that the  $\alpha_{2A}$ AR response in hippocampus was PTX-sensitive, indicating a role for the  $G_{i/o}$  family. The small residual effect after PTX treatment ( $<1/3$  of the control response) could be due to incomplete modification of the  $G_{i/o}$  proteins during the 7- to 8-h pretreatment period, because many studies use an overnight ( $>12$  h) treatment with PTX. Alternatively, a non-PTX-sensitive protein like  $G_z$  could play a small role.

To further examine which  $G_{i/o}$  subtype(s) can mediate EPI's effect, mice with knock-in mutant RGS-insensitive  $G_{\alpha_o}$  or  $G_{\alpha_{i2}}$  were used. The knock-in mice differ from WT only in the presence of the G184S mutation, which prevents RGS binding to the  $G\alpha$  subunit and the subsequent GTPase acceleration (Fu et al., 2004; Huang et al., 2006). Consequently, this mutation results in prolonged and enhanced activation of the modified G protein, which increases signal transduction by both the  $\alpha$  and  $\beta\gamma$  subunits derived from that G protein. The heterozygous  $G_{\alpha_o}$  RGS-insensitive [ $G_{\alpha_o}(+/G184S)$ ] knock-in animals showed a 7-fold leftward shift of the EPI dose-response curve (2.5 versus 19 nM), whereas there was no significant difference in potency between the heterozygous  $G_{\alpha_{i2}}$  RGS-insensitive mouse (19 nM) and its control (23 nM). The pronounced effect even in the heterozygous mouse is not surprising. RGS proteins can accelerate G protein deactivation nearly 1000-fold (Mukhopadhyay and Ross, 1999; Lan et al., 2000), dramatically suppressing G protein signaling. The G184S mutation eliminates this negative regulatory effect, so it produces a gain-of-function phenotype in

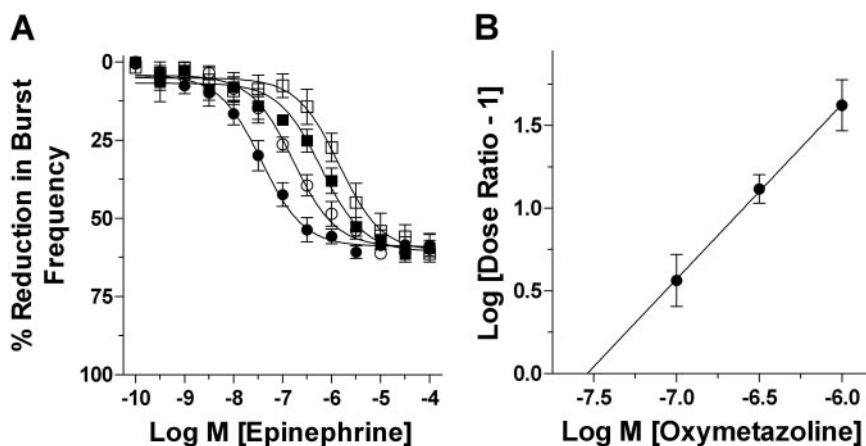


**Fig. 6.** Schild regression analysis using the selective  $\alpha_{2A}$ AR ligand oxymetazoline in slices from  $\alpha_{2C}$ AR-KO mice. A, consecutive EPI concentration-response curves demonstrate a concentration-dependent effect of the selective  $\alpha_{2A}$ AR ligand, oxymetazoline, on the EPI-mediated inhibition of hippocampal CA3 epileptiform activity in brain slices from  $\alpha_{2C}$ AR-KO mice. Pretreatment with 100 nM ( $\circ$ ), 300 nM ( $\blacksquare$ ), and 1000 nM ( $\square$ ) concentrations of this antagonist produced consecutive parallel rightward shifts of the EPI curve that were significantly different from control ( $\bullet$ ) ( $EC_{50}$  =  $205 \pm 48$ ,  $738 \pm 267$ , and  $2317 \pm 980$  nM, respectively, versus  $33 \pm 9$  nM for control). B, using dose ratios calculated from individual experiments illustrated in A, a Schild plot was created generating a regression slope equaling  $1.16 \pm 0.12$  and an  $x$ -intercept correlating to a  $pK_b$  value of 7.50,  $n = 7$  animals. This  $pK_b$  value matched the binding affinity of oxymetazoline ( $pK_i = 7.49$ ) for the mouse  $\alpha_{2A}$ AR, but not the mouse  $\alpha_{2B}$ AR ( $pK_i = 5.92$ ) (Chruscinski et al., 1992) or mouse  $\alpha_{2C}$ AR ( $pK_i = 6.96$ ) (Link et al., 1992).

which even half of the G protein removed from this suppression could produce a marked increase in signaling. Previous studies with the G $\alpha_{i2}^{G184S}$  knock-in mutants have also shown significant effects in heterozygous mice (Huang et al., 2006). Thus, these results show that RGS proteins play a key role in regulating the  $\alpha_{2A}$ AR-mediated hippocampal CA3 antiepileptiform effect and suggest that the G $\alpha_o$  subtype of G $\gamma_i$  proteins is involved in the signaling mechanism, whereas G $\alpha_{i2}$  seems not to be. At this stage, we cannot rule out a contribution from other

pertussis toxin-sensitive G proteins such as G $\alpha_{i1}$  or G $\alpha_{i3}$ , but the evidence clearly indicates that G $\alpha_o$  does play a role.

Several important questions remain. Although the G $\alpha_o$  RGS-insensitive mouse shows that an RGS protein is involved in this system, it does not reveal which of the 20-plus RGS proteins (Hollinger and Hepler, 2002; Neubig and Sidarovski, 2002) are important. Given that nearly 15 different RGS proteins can function as a GTPase-activating protein for G $\alpha_o$ , it may be difficult to establish which one(s) are involved. Furthermore, it is possible that more than one RGS protein may work in a redundant manner in this system. That said, the RGS7 family of RGS proteins (RGS6, 7, 9, and 11) represent intriguing candidates because they are relatively selective for G $\alpha_o$  in vitro (Lan et al., 2000). A second question is whether the same enhancement of  $\alpha_{2A}$ AR agonist anticonvulsant actions will be seen in vivo. Studies are currently underway to assess this question.

The present study suggests two strategies that may provide improved therapeutics for adrenergic agonist anticonvulsants. First, an  $\alpha_{2A}$ AR agonist that can selectively activate G $\alpha_o$  versus G $\alpha_{i2}$  or other G $\gamma_i$  family members could lead to improved potency and/or reduced side effects. It would also be important for such a compound to preferentially activate the  $\alpha_{2A}$ ARs on target neurons over  $\alpha_{2A}$ AR autoreceptors that would decrease NE release. This could be achieved by a "functionally selective" (Urban et al., 2007)  $\alpha_{2A}$ AR agonist. Second, RGS proteins have been implicated as potential therapeutic targets. Several peptide (Jin et al., 2004; Young et al., 2004; Roof et al., 2006) and nonpeptide (Roman et al., 2007) RGS inhibitors have been described. To date, none are active in vivo for pharmacological studies, but the identification of the involved RGS protein and the creation of an inhibitor that could target it could either produce anticonvulsant effects through endogenous NE or potentially reduce side ef-

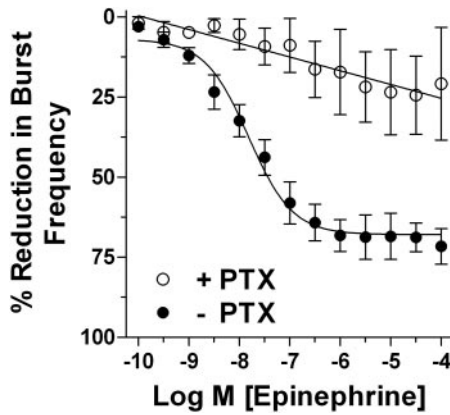


**Fig. 7.** PTX reduces the EPI-mediated inhibition of hippocampal CA3 epileptiform bursts. Extracellular field potential recordings of epileptiform burst frequency were used to generate concentration-response curves using increasing amounts of EPI in untreated control slices (●) or slices treated (○) with 5  $\mu$ g/ml PTX for 7 to 8 h. Concentration-response curves for EPI were plotted as a percentage of decrease (reduction) in epileptiform burst frequency. The mean concentration-response curve for nontreated control slices was fit best by a nonvariable sigmoidal model with a calculated EC $_{50}$  value of 12  $\pm$  3.9 nM and an efficacy of 74  $\pm$  6.1% ( $n$  = 13 slices from 6 animals). In contrast, for PTX-treated slices from these same mice, the mean concentration-response curve was fit best by a linear regression line and had an efficacy of 24  $\pm$  13% ( $n$  = 12 slices from 6 animals).

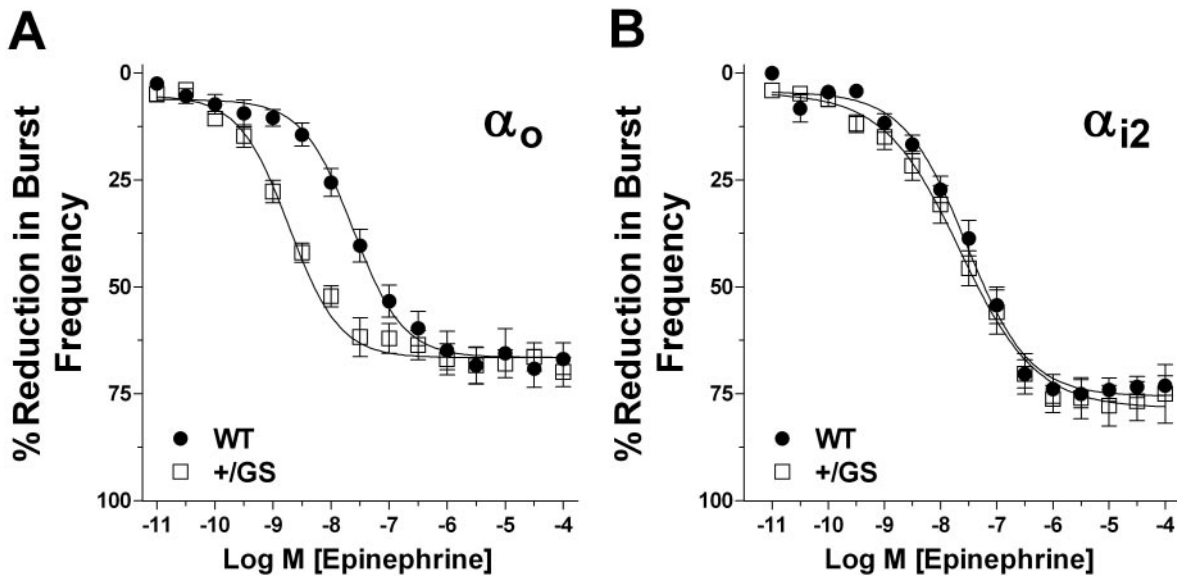


**Fig. 8.** EPI-mediated inhibition of hippocampal CA3 epileptiform bursts is significantly enhanced in brain slices from G $\alpha_o$ +GS mice but not G $\alpha_{i2}$ +GS mice. Extracellular field potential recordings were used to generate concentration-response curves using increasing amounts of EPI (●) in the presence of 30  $\mu$ M timolol and 0.5  $\mu$ M desipramine. Concentration-response curves for EPI were plotted as a percent reduction in epileptiform burst frequency. Each individual experiment best fit to a nonvariable sigmoidal curve. A, there was a significant difference in the potencies (EC $_{50}$  values) calculated for EPI in brain slices from G $\alpha_o$ +GS mice (□) (2.5  $\pm$  0.9 nM,  $n$  = 23 slices from 6 animals) versus litter mate control mice (●) (19  $\pm$  5 nM,  $n$  = 21 slices from 6 animals). B, in contrast, the EPI-mediated inhibition of epileptiform activity was unchanged in brain slices from G $\alpha_{i2}$ +GS mice (□) (19  $\pm$  5 nM,  $n$  = 32 slices from 6 animals) compared with WT control mice (●) (23  $\pm$  7 nM,  $n$  = 22 slices from 8 animals). There was no significant difference in the efficacy of EPI among these four groups (G $\alpha_o$ +GS, 74  $\pm$  3.8%; G $\alpha_o$  litter mate control, 74  $\pm$  4.4%; G $\alpha_{i2}$ +GS, 73  $\pm$  2.8%; G $\alpha_{i2}$  WT control, 75  $\pm$  3.6%).



fects on the treatment with  $\alpha_{2A}$ AR-selective agonists in patients with epilepsy.

In summary, we have defined the receptor ( $\alpha_{2A}$ AR), a G protein ( $G\alpha_o$ ), and a regulatory mechanism (RGS proteins) that are important for the antiepileptiform actions of NE and EPI in the hippocampus, a key site of seizure activity in many patients. These advances provide a theoretical rationale for future, novel therapeutic approaches.

#### Acknowledgments

We thank Sarah J. Boese, Chris W. D. Jurgens, Brandi A. Kaster, Jasmine J. O'Brien, and Danielle D. Schlosser for help with the experiments, Karen L. Cisek for assistance in editing the manuscript, and Dr. James E. Porter for advice about data acquisition and Schild regression analysis.

#### References

- Arunlakshana O and Schild HO (1959) Some quantitative uses of drug antagonists. *Br J Pharmacol* **14**:48–58.
- Berman DM, Wilkie TM, and Gilman AG (1996) GAIP and RGS4 are GTPase-activating proteins for the G<sub>i</sub> subfamily of G protein  $\alpha$  subunits. *Cell* **86**:445–452.
- Bylund DB (1988) Subtypes of  $\alpha_2$ -adrenoceptors: pharmacological and molecular evidence converge. *Trends Pharmacol Sci* **9**:356–361.
- Bylund DB, Eikenberg DC, Hieble JP, Langer SZ, Lefkowitz RJ, Minneman KP, Molinoff PB, Ruffolo RR Jr, and Trendelenburg U (1994) International Union of Pharmacology nomenclature of adrenoceptors. *Pharmacol Rev* **46**:121–136.
- Chruscinski AJ, Link RE, Daunt DA, Barsh GS, and Kobilka BK (1992) Cloning and expression of the mouse homolog of the human  $\alpha_2$ -C2 adrenergic receptor. *Biochem Biophys Res Commun* **186**:1280–1287.
- Clark MJ, Harrison C, Zhong H, Neubig RR, and Traynor JR (2003) Endogenous RGS protein action modulates  $\mu$ -opioid signaling through  $G\alpha_o$ . *J Biol Chem* **278**:9418–9425.
- Clark MJ, Linderman JJ, and Traynor JR (2008) Endogenous regulators of G protein signaling differentially modulate full and partial  $\mu$ -opioid agonists at adenylyl cyclase as predicted by a collision coupling model. *Mol Pharmacol* **73**:1538–1548.
- Devauges V and Sara SJ (1991) Memory retrieval enhancement by locus coeruleus stimulation: evidence for mediation by  $\beta$ -receptors. *Behav Brain Res* **43**:93–97.
- Fu Y, Huang X, Zhong H, Mortensen RM, D'Alecy LG, and Neubig RR (2006) Endogenous RGS proteins and  $G\alpha$  subtypes differentially control muscarinic and adenosine-mediated chronotropic effects. *Circ Res* **98**:659–666.
- Fu Y, Zhong H, Nanamori M, Mortensen RM, Huang X, Lan K, and Neubig RR (2004) RGS-insensitive G-protein mutations to study the role of endogenous RGS proteins. *Methods Enzymol* **389**:229–243.
- Gilman AG (1987) G proteins: Transducers of receptor-generated signals. *Annu Rev Biochem* **56**:615–649.
- Giorgi FS, Pizzanelli C, Biagioni F, Murri L, and Fornai F (2004) The role of norepinephrine in epilepsy: from the bench to the bedside. *Neurosci Biobehav Rev* **28**:507–524.
- Hillman KL, Knudson CA, Carr PA, Doze VA, and Porter JE (2005) Adrenergic receptor characterization of CA1 hippocampal neurons using real time single cell RT-PCR. *Brain Res Mol Brain Res* **139**:267–276.
- Hollinger S and Hepler JR (2002) Cellular regulation of RGS proteins: modulators and integrators of G protein signaling. *Pharmacol Rev* **54**:527–559.
- Hopkins WF and Johnston D (1988) Noradrenergic enhancement of long-term potentiation at mossy fiber synapses in the hippocampus. *J Neurophysiol* **59**:667–687.
- Huang X, Fu Y, Charbeneau RA, Saunders TL, Taylor DK, Hankenson KD, Russell MW, D'Alecy LG, and Neubig RR (2006) Pleiotropic phenotype of a genomic knock-in of an RGS-insensitive G184S Gna2 allele. *Mol Cell Biol* **26**:6870–6879.
- Institute of Laboratory Animal Resources (1996) *Guide for the Care and Use of Laboratory Animals*, 7th ed. Institute of Laboratory Animal Resources, Commission on Life Sciences, National Research Council, Washington DC.
- Janumpalli S, Butler LS, MacMillan LB, Limbird LE, and McNamara JO (1998) A point mutation (D79N) of the  $\alpha_2A$  adrenergic receptor abolishes the antiepileptogenic action of endogenous norepinephrine. *J Neurosci* **18**:2004–2008.
- Jin Y, Zhong H, Omnaas JR, Neubig RR, and Mosberg HI (2004) Structure-based design, synthesis, and pharmacologic evaluation of peptide RGS4 inhibitors. *J Pept Res* **63**:141–146.
- Jurgens CW, Boese SJ, King JD, Pyle SJ, Porter JE, and Doze VA (2005) Adrenergic receptor modulation of hippocampal CA3 network activity. *Epilepsy Res* **66**:117–128.
- Jurgens CW, Hammad HM, Lichter JA, Boese SJ, Nelson BW, Goldenstein BL, Davis KL, Xu K, Hillman KL, Porter JE, et al. (2007)  $\alpha_{2A}$  Adrenergic receptor activation inhibits epileptiform activity in the rat hippocampal CA3 region. *Mol Pharmacol* **71**:1572–1581.
- Kesner RP, Lee I, and Gilbert P (2004) A behavioral assessment of hippocampal function based on a subregional analysis. *Rev Neurosci* **15**:333–351.
- Lan KL, Sarvazyan NA, Taussig R, Mackenzie RG, DiBello PR, Dohlman HG, and Neubig RR (1998) A point mutation in  $G\alpha_o$  and  $G\alpha_{i1}$  blocks interaction with regulator of G protein signaling proteins. *J Biol Chem* **273**:12794–12797.
- Lan KL, Zhong H, Nanamori M, and Neubig RR (2000) Rapid kinetics of regulator of G-protein signaling (RGS)-mediated  $G\alpha_i$  and  $G\alpha_o$  deactivation. *J Biol Chem* **275**:33497–33503.
- Link R, Daunt D, Barsh G, Chruscinski A, and Kobilka B (1992) Cloning of two mouse genes encoding  $\alpha_2$ -adrenergic receptor subtypes and identification of a single amino acid in the mouse  $\alpha_2$ -C10 homolog responsible for an interspecies variation in antagonist binding. *Mol Pharmacol* **42**:16–27.
- MacMillan LB, Lakhiani PP, Hein L, Piascik M, Guo TZ, Lovinger D, Maze M, and Limbird LE (1998) In vivo mutation of the  $\alpha_{2A}$ -adrenergic receptor by homologous recombination reveals the role of this receptor subtype in multiple physiological processes. *Adv Pharmacol* **42**:493–496.
- Mortensen RM, Conner DA, Chao S, Geisterfer-Lowrance AA, and Seidman JG (1992) Production of homozygous mutant ES cells with a single targeting construct. *Mol Cell Biol* **12**:2391–2395.
- Mukhopadhyay S and Ross EM (1999) Rapid GTP binding and hydrolysis by  $G_i$  promoted by receptor and GTPase-activating proteins. *Proc Natl Acad Sci U S A* **96**:9539–9544.
- Neubig RR and Siderovski DP (2002) Regulators of G-protein signaling as new central nervous system drug targets. *Nat Rev Drug Discov* **1**:187–197.
- Newman-Tancredi A, Nicolas JP, Audinot V, Gavaudan S, Verri le L, Touzard M, Chaput C, Richard N, and Millan MJ (1998) Actions of  $\alpha_2$  adrenoceptor ligands at  $\alpha_{2A}$  and 5-HT<sub>1A</sub> receptors: the antagonist, atipamezole, and the agonist, dexmedetomidine, are highly selective for  $\alpha_{2A}$  adrenoceptors. *Naunyn-Schmiedeberg Arch Pharmacol* **358**:197–206.
- Offermanns S (2003) G-proteins as transducers in transmembrane signaling. *Prog Biophys Mol Biol* **83**:101–130.
- Pupo AS and Minneman KP (2001) Adrenergic pharmacology: Focus on the central nervous system. *CNS Spectr* **6**:656–662.
- Roman DL, Talbot JN, Roof RA, Sunahara RK, Traynor JR, and Neubig RR (2007) Identification of small-molecule inhibitors of RGS4 using a high-throughput flow cytometry protein interaction assay. *Mol Pharmacol* **71**:169–175.
- Roof RA, Jin Y, Roman DL, Sunahara RK, Ishii M, Mosberg HI, and Neubig RR (2006) Mechanism of action and structural requirements of constrained peptide inhibitors of RGS proteins. *Chem Biol Drug Des* **67**:266–274.
- Schwartzkroin PA (1986) Hippocampal slices in experimental and human epilepsy. *Adv Neurol* **44**:991–1010.
- Szot P, Lester M, Laughlin ML, Palmiter RD, Liles LC, and Weinschenker D (2004) The anticonvulsant and proconvulsant effects of  $\alpha_2$ -adrenoceptor agonists are mediated by distinct populations of  $\alpha_{2A}$ -adrenoceptors. *Neuroscience* **126**:795–803.
- Urban JD, Clarke WP, von Zastrow M, Nichols DE, Kobilka B, Weinstein H, Javitch JA, Roth BL, Christopoulos A, Sexton PM, et al. (2007) Functional selectivity and classical concepts of quantitative pharmacology. *J Pharmacol Exp Ther* **320**:1–13.
- Watson N, Lindner ME, Druey KM, Kehrl JH, and Blumberg P (1996) RGS family members: GTPase-activating proteins for heterotrimeric G-protein  $\alpha$ -subunits. *Nature* **383**:172–175.
- Weinschenker D and Szot P (2002) The role of catecholamines in seizure susceptibility: new results using genetically engineered mice. *Pharmacol Ther* **94**:213–233.
- Young KH, Wang Y, Bender C, Ajit S, Ramirez F, Gilbert A, and Nieuwenhuisen BW (2004) Yeast-based screening for inhibitors of RGS proteins. *Methods Enzymol* **389**:277–301.
- Zhong H and Neubig RR (2001) Regulator of G protein signaling proteins: novel multifunctional drug targets. *J Pharmacol Exp Ther* **297**:837–845.

**Address correspondence to:** Dr. Van A. Doze, Department of Pharmacology, Physiology and Therapeutics, School of Medicine and Health Sciences, University of North Dakota, 501 North Columbia Road, Stop 9037, Grand Forks, ND 58202-9037. E-mail: vdoze@medicine.nodak.edu